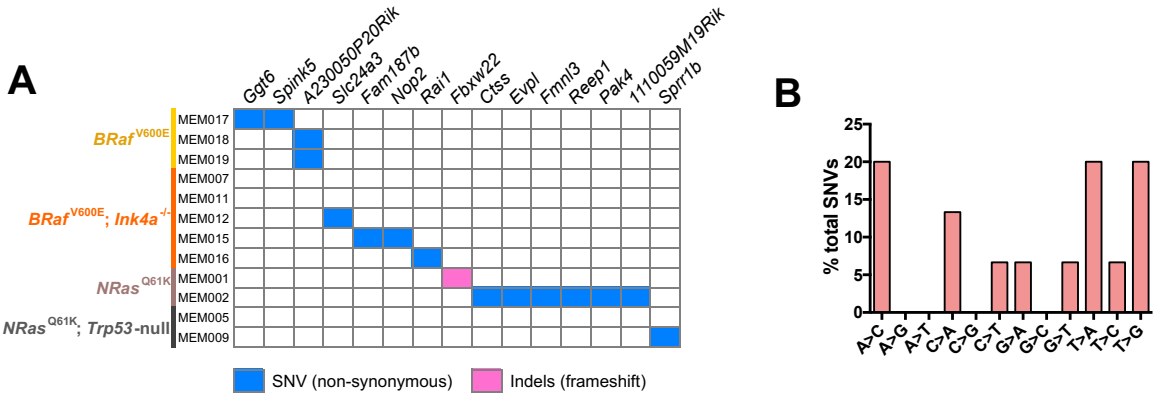

Supplementary Figure 1: Whole-exome sequencing of murine melanoma genomes. (**A**) Validated SNAs and indels and (**B**) mutational signature from 12 mouse melanomas of genetically-defined origins.

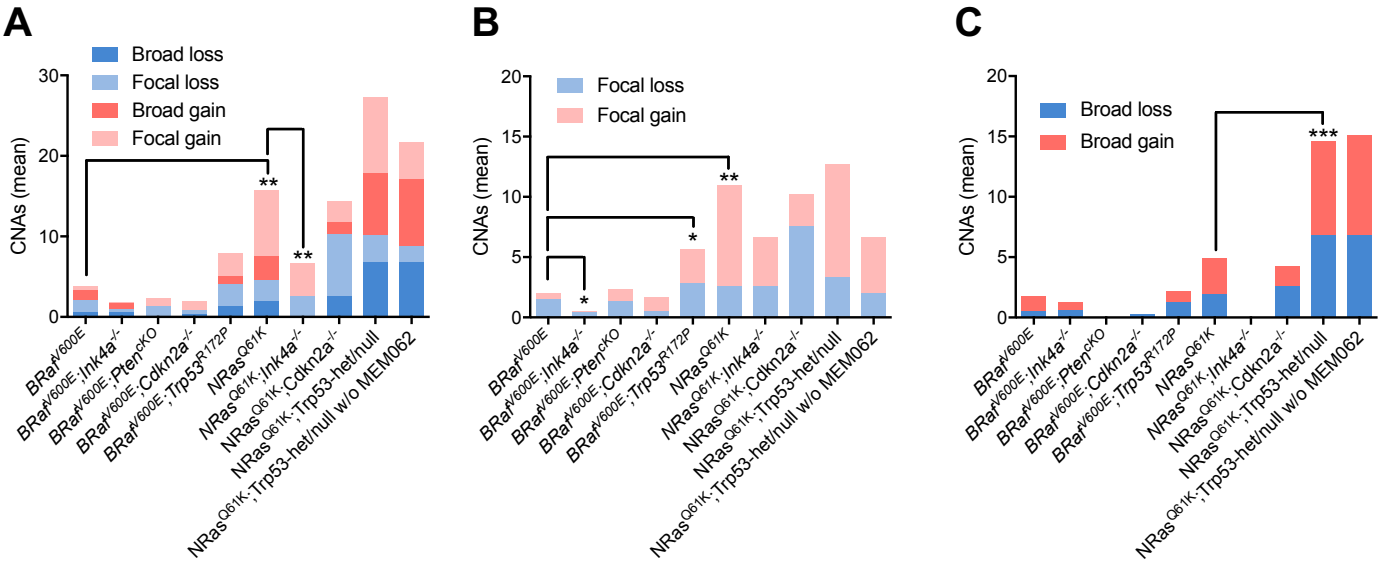

Supplementary Figure 2: Graphs showing the average number of both focal and broad CNAs (**A**) and separate comparisons for only focal (**B**) and broad (**C**) CNAs per experimental group. The *NRas^{Q61K};Trp53-het/null* group is shown with and without MEM062 sample to clarify that the increase of CNAs in this sample is purely because of focal CNAs. Significance determined by unpaired two-sided *t*-test (* $P \leq 0.05$; ** $P \leq 0.01$; *** $P \leq 0.001$).

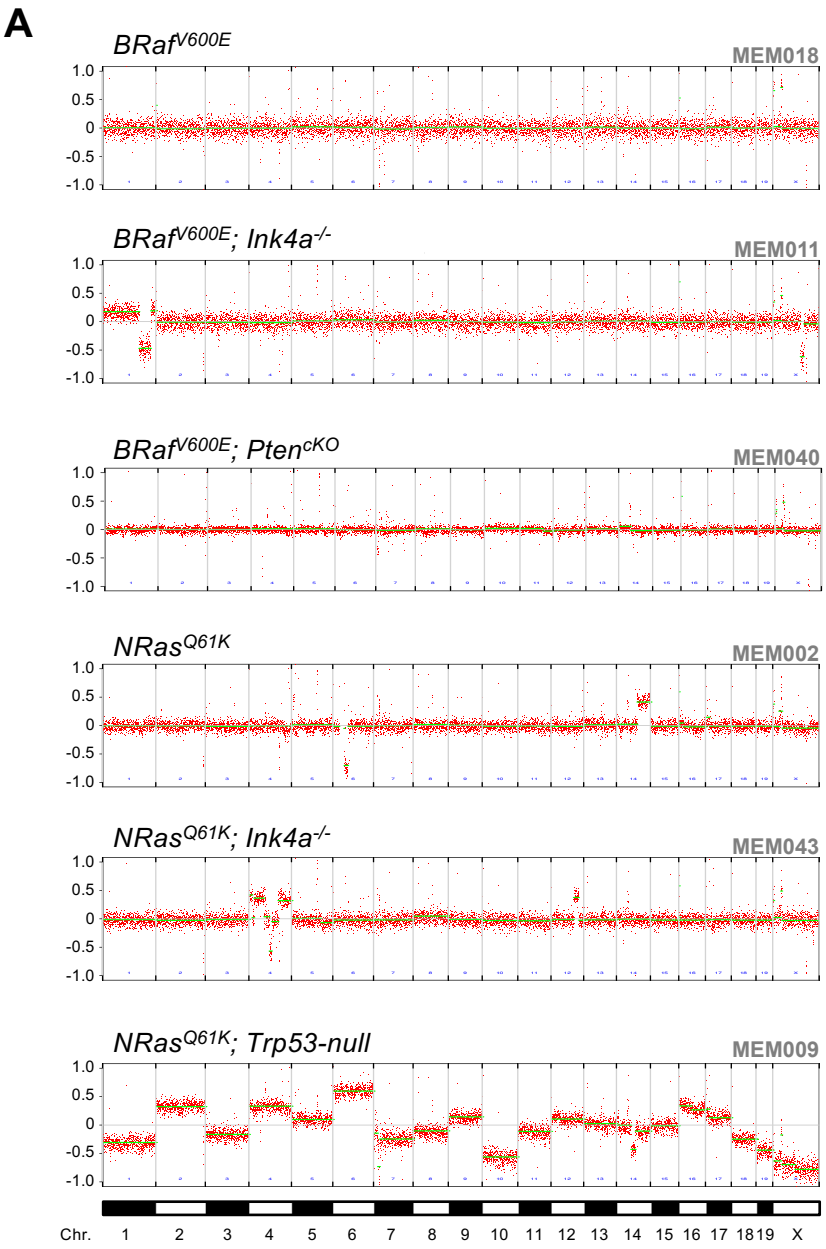

Supplementary Figure 3: Representative plots of shallow WGS from murine genetically-induced melanomas with the indicated genotypes (**A**) and from a human melanoma (**B**).

Supplementary Figure 4

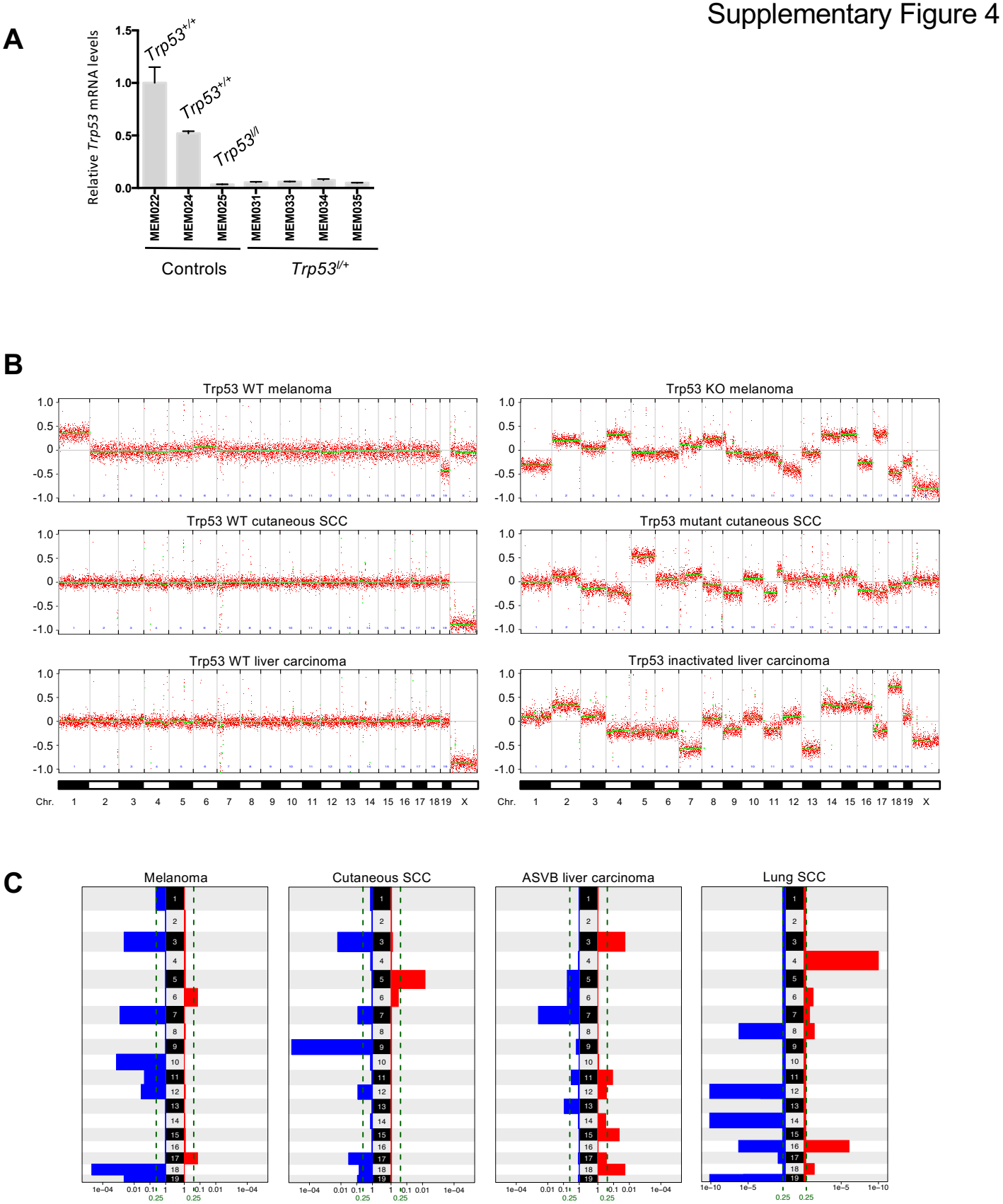

Supplementary Figure 4: p53 loss leads to aneuploidy. (**A**) *Trp53* mRNA levels assessed by RT-qPCR in melanoma samples with the indicated genotypes. (**B**) Shallow WGS plots of representative *Trp53* wild-type (left panels) or inactivated *Trp53* (right panels) murine melanoma, cutaneous squamous cell carcinoma (SCC) and liver carcinoma. (**C**) GISTIC analysis of recurrent whole-chromosome amplification (red) or deletion (blue) in Trp53 inactivated tumors of various origins, including melanoma, cutaneous SCC, liver carcinoma and lung carcinoma. The lung SCC plot was adapted from McFadden *et al*. (27).

Supplementary Figure 5

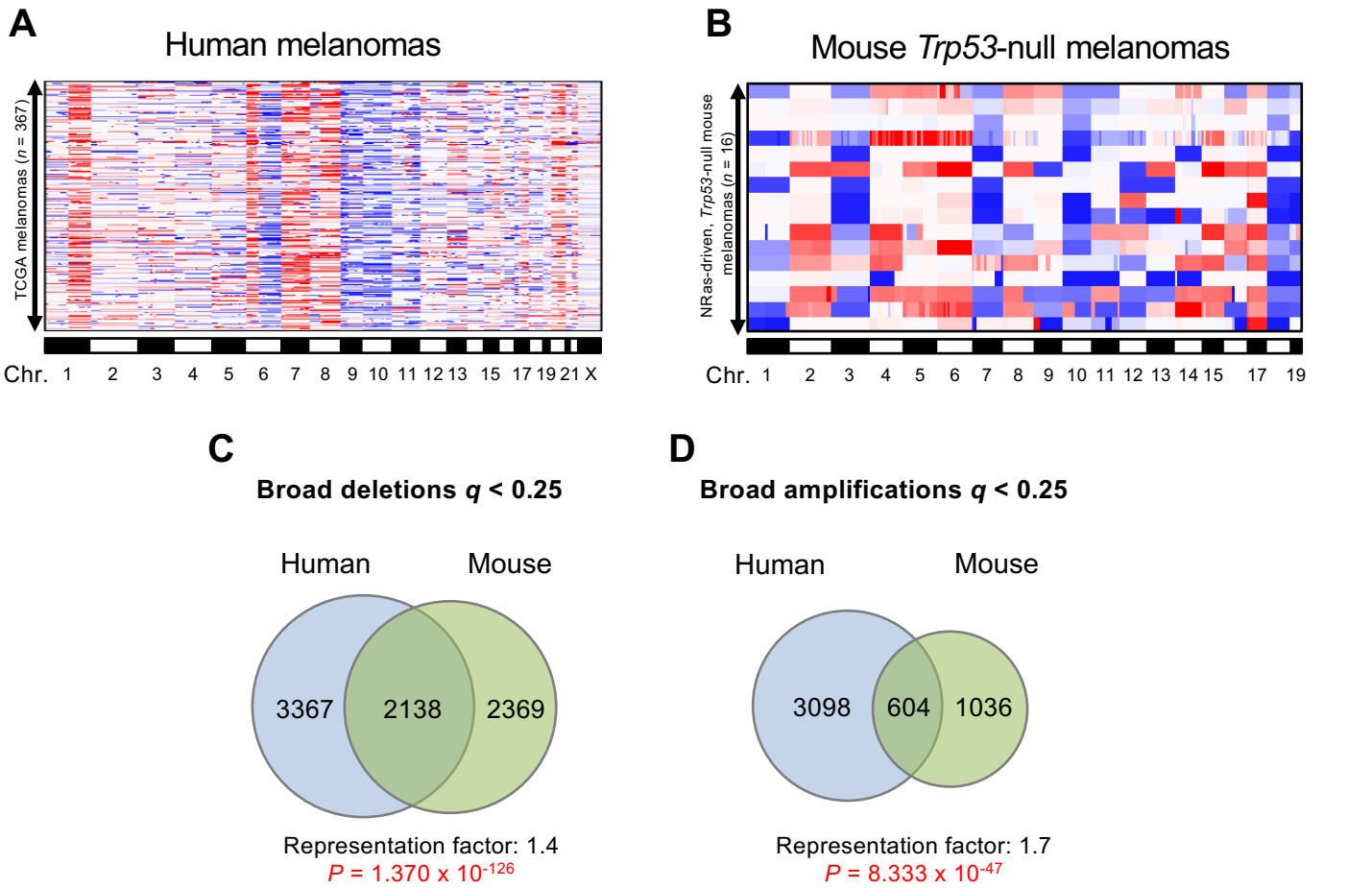

Supplementary Figure 5: CNA Profiles of NRas-driven, *Trp53*-null melanomas recapitulate CNAs from human melanomas. (**A-B**) Heat maps of CNAs in human melanomas from the TCGA cohort (*n* = 367; **A**) and NRas-driven, *Trp53*-null murine melanomas (*n* = 16; **B**). (**C-D**) Statistical significance of the overlap between gene orthologues targeted by broad CNAs in human *vs.* murine melanomas. Human and mouse orthologues (*n* = 16,728 genes) targeted by recurrent broad deletions (*q* < 0.25; **C**) or amplifications (*q* < 0.25; **D**) were analyzed. Statistical significance of overlapping gene sets was determined by a hypergeometric distribution test.

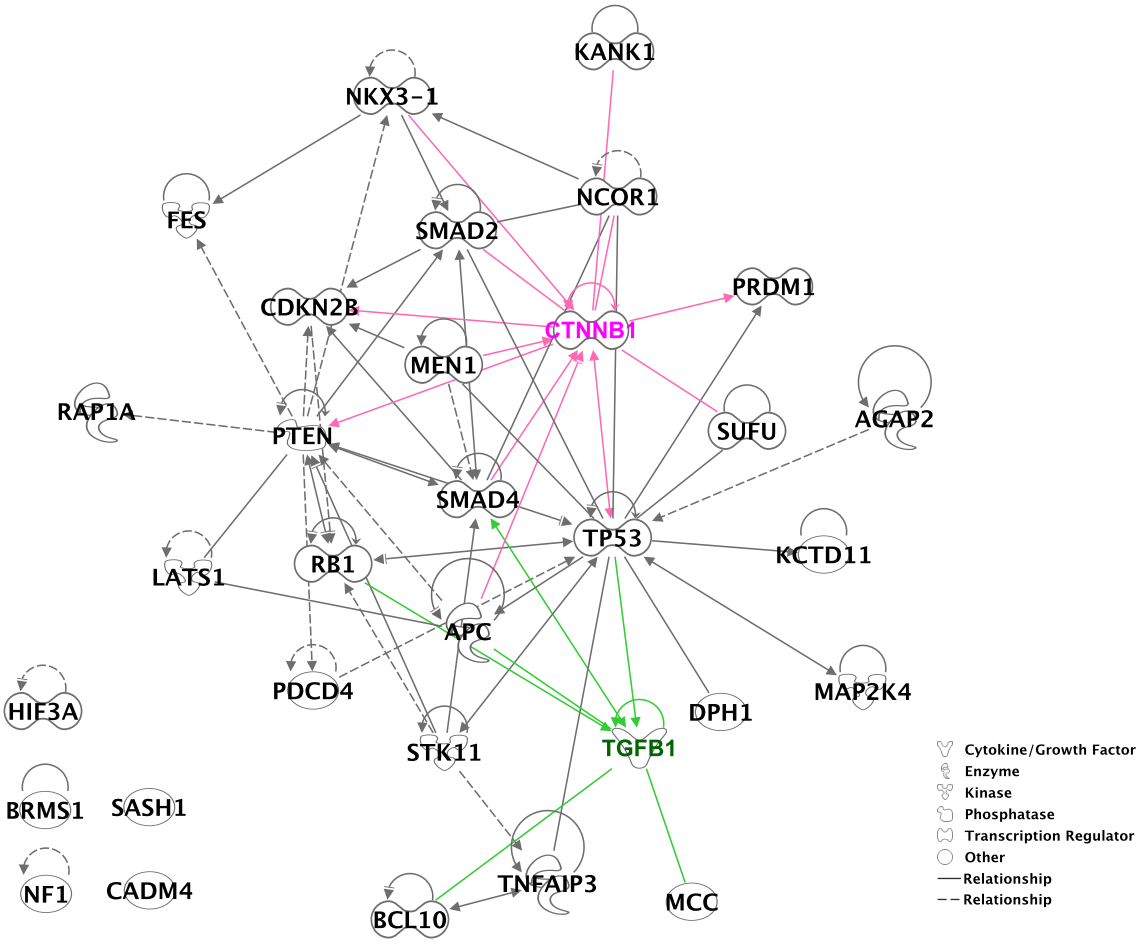

Supplementary Figure 6: Pathway analysis of putative melanoma TSGs. IPA analysis of 30 selected genes which are targeted by deletions in murine melanomas. 76% of these genes are functionally linked; many of these genes are connected to known melanoma driver and progression pathways such the WNT/*β*-catenin, p53 and TGF-beta signaling pathways.

Supplementary Figure 7

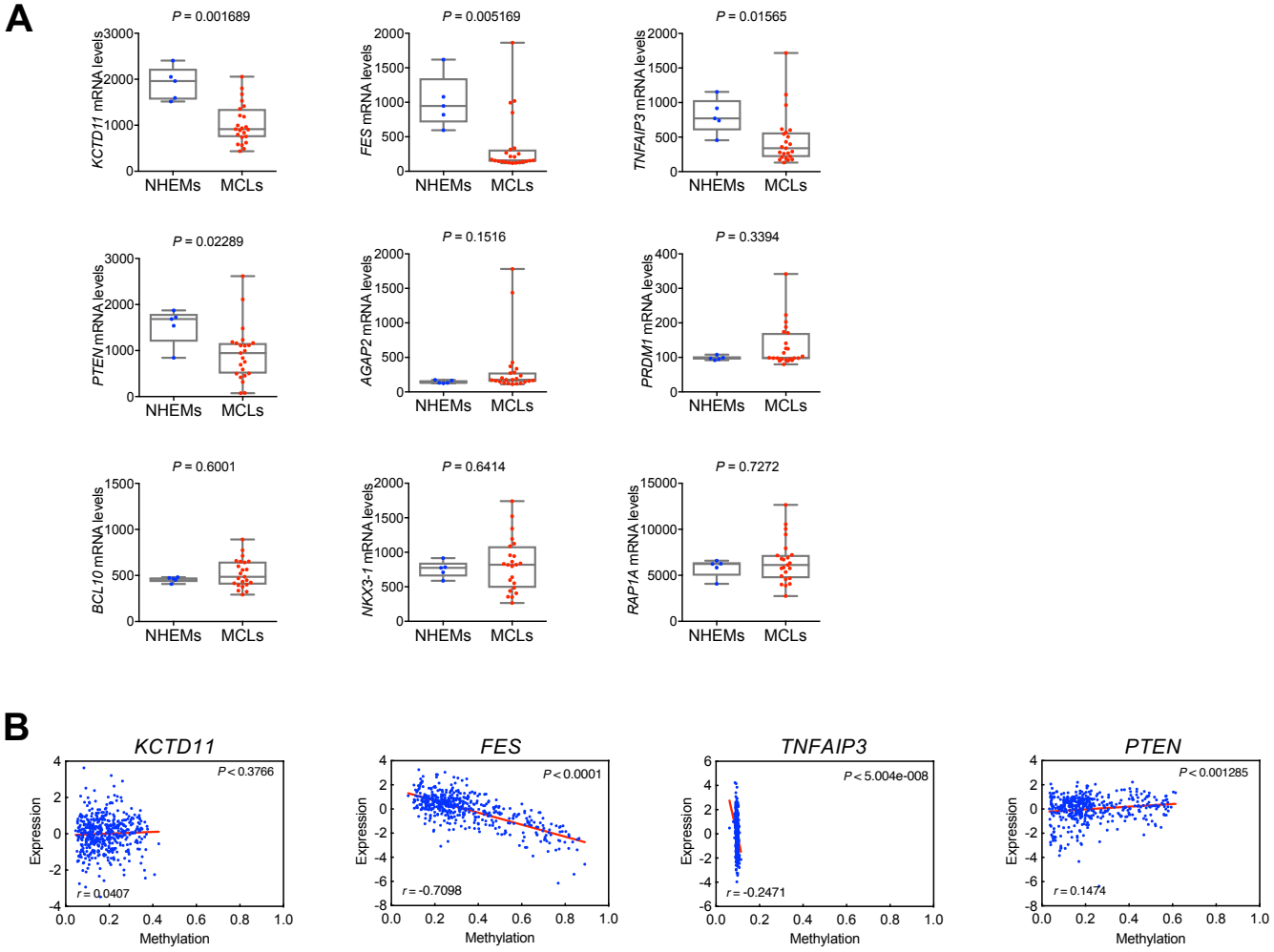

Supplementary Figure 7: Expression of 9 putative TSGs in human melanomas. (**A**) Expression profiles of putative TSGs in normal human melanocytes (NHEMs) and melanoma cell lines (MCLs) as assessed by the analysis of the microarray dataset described in Rambow *et al*. (ref. 38). (**B**) Correlation plots between mRNA levels and the average methylation of CpGs in the vicinity of the TSS of selected putative TSGs. Pearson r and significance is indicated. Statistical significance was determined by unpaired two-sided *t*-test (**A**) and Pearson correlation (**B**).

Supplementary Figure 8

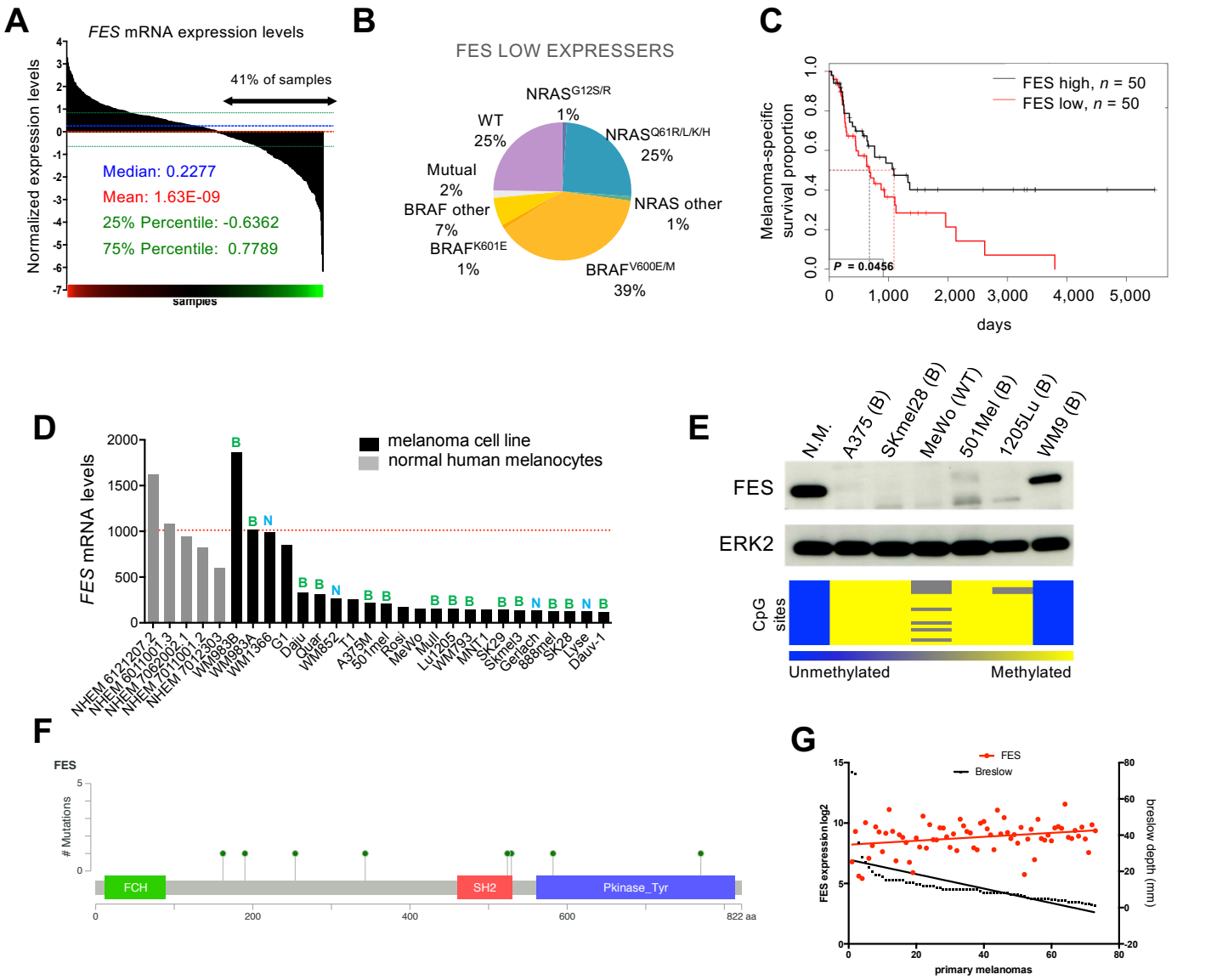

Supplementary Figure 8: FES expression in human melanomas. (**A**) Expression profile plot of *FES* mRNA in the TCGA cohort of human melanomas. (**B**) BRAF and NRAS mutational status of FES low expressing melanomas from TCGA-SKCM (samples from (**A**) with expression below the mean). (**C**) Survival curve of FES-high and FES-low (n = 50 per group) expressing melanoma patients. (**D**) Expression of FES in normal human melanocytes (NHEM; shown as grey columns) and melanoma cell lines (shown as black columns) as assessed by analysis of the microarray dataset described by Rambow *et al*. (ref. 38). The $BRAF^{V600E}$ (B) and $NRAS^{Q61K,L,R}$ (N) mutational status of cell lines is indicated. The red dotted line indicates mean value of NHEM. (**E**) Western blotting analysis of FES in melanoma cell lines and normal human melanocyte culture (N.M.). The methylation profile of the CpG island located close to the TSS of *FES* is shown below. The $BRAF^{V600E}$ (B) and $NRAS^{Q61K,L,R}$ (N) mutational status of cell lines is indicated in brackets. (**F**) cBioPortal visualization of the mutations targeting the *FES* locus in TCGA-SKCM cohort. (**G**) Plot showing the log_2-transformed expression values of FES in relation with the Breslow depth of human melanomas from TCGA cohort. Statistical significance was determined using Mantel-Cox test (**B**).

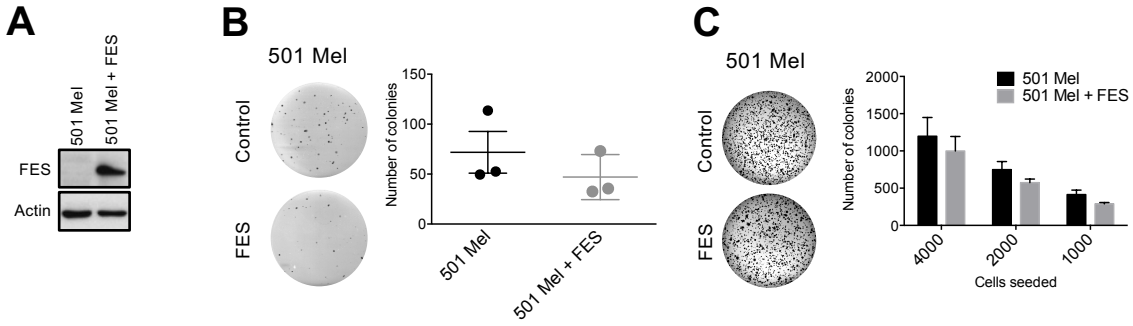

Supplementary Figure 9: Restoration of FES expression in the 501 Mel human melanoma cell line. (**A**) Western blot analysis of FES in 501 Mel cell line with overexpression of FES. Actin served as a loading control. (**B**) Clonogenic assay of 501 Mel cells with and without expression of exogenous FES. Error bars, mean ± s.e.m. (*n* = 3 biological replicates per group). (**C**) Soft agar assay of 501 Mel cells with and without expression of exogenous FES. Error bars, mean ± s.e.m. (*n* = 3 biological replicates per group).

Supplementary Figure 10

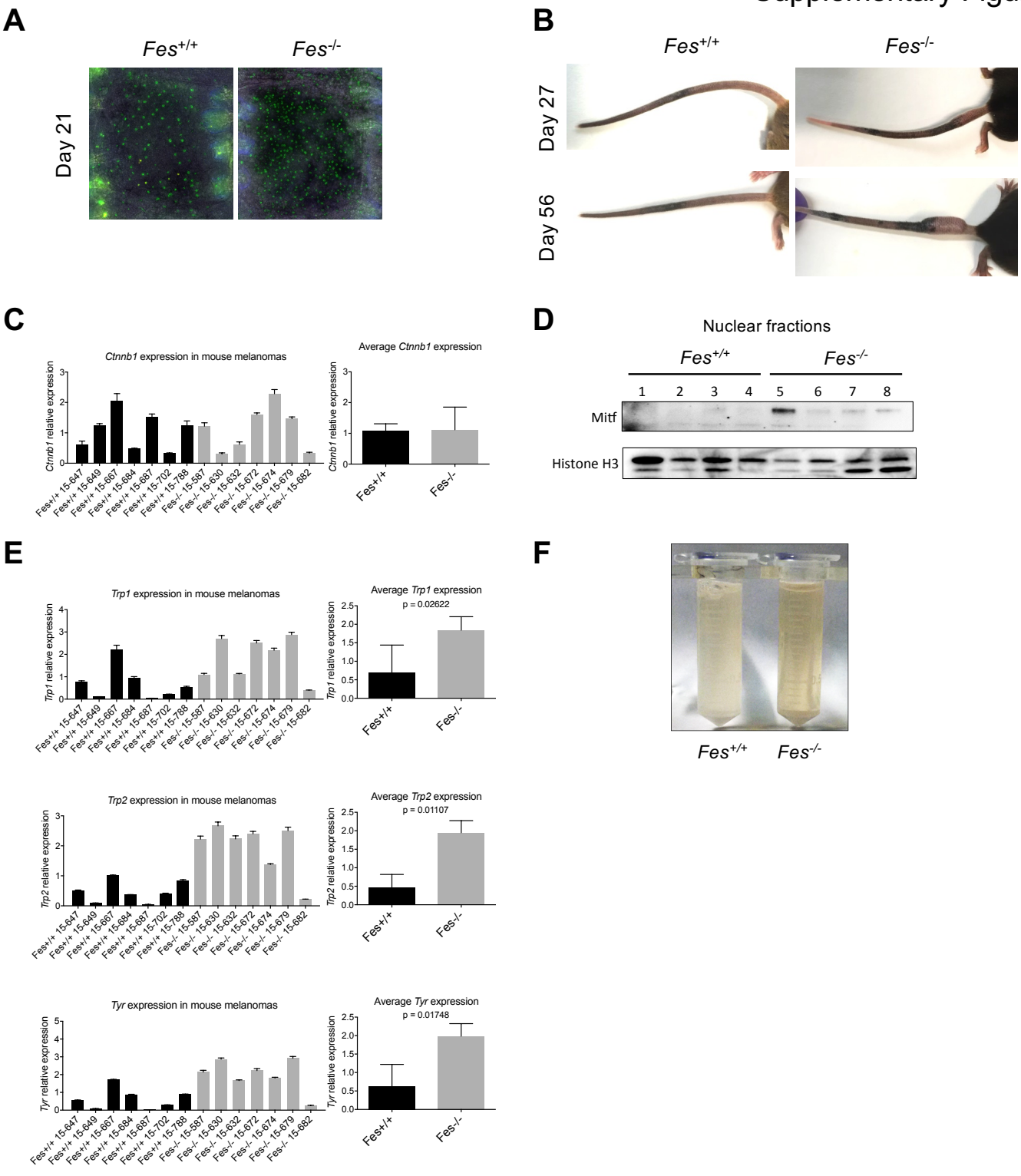

Supplementary Figure 10: Increased pigmentation in *FES* KO melanomas. (**A**) Representative pictures of epidermal whole mount displaying the area of individual tail scales at day 21 after 4-HT treatment. Melanoma cells are stained using gp100 antibody (green). (**B**) Representative pictures of tails of *Tyr::Cre*$^{ERT2/°}$; *Braf*$^{CA/+}$; *Pten*$^{fl/fl}$ mice either *Fes*$^{+/+}$ or *Fes*$^{-/-}$ at day 27 and 56 post-topical treatment of the tail with 5 mM of 4-HT. (**C**) RT-qPCR analysis showing expression of *Ctnnb1* in *Fes*$^{+/+}$ or *Fes*$^{-/-}$ melanomas. Error bars, mean ± s.d. (*n* = 3). The graph on the right shows average value per group. Error bars, mean ± s.e.m. (*n* = 7 per group). (**D**) Western blotting of MITF and Histone H3 (as loading control) in nuclear extracts from *Fes*$^{+/+}$ or *Fes*$^{-/-}$ melanomas. (**E**) Expression of key pigmentation genes *Trp1*, *Trp2* and *Tyr* in *Fes*$^{+/+}$ or *Fes*$^{-/-}$ melanomas. Error bars, mean ± s.d. (*n* = 3). The graph on the right shows average value per group. Error bars, mean ± s.e.m. (*n* = 7 per group). (**F**) Representative images highlighting the difference in pigmentation intensity in *Fes*$^{+/+}$ and *Fes*$^{-/-}$ total protein extracts. The statistical significance was determined using Mann-Whitney *U*-test (**C, E**).